

Supplement of **“The evolution of future Antarctic surface melt using PISM-dEBM-simple”**

Julius Garbe^{1,2}, Maria Zeitz^{1,2}, Uta Krebs-Kanzow³, and Ricarda Winkelmann^{1,2}

¹Potsdam Institute for Climate Impact Research (PIK), Member of the Leibniz Association, P.O. Box 60 12 03, 14412 Potsdam, Germany

²University of Potsdam, Institute of Physics and Astronomy, Karl-Liebknecht-Str. 24-25, 14476 Potsdam, Germany

³Alfred Wegener Institute Helmholtz Centre for Polar and Marine Research, Bremerhaven, Germany

Correspondence: Julius Garbe (julius.garbe@pik-potsdam.de)

List of supplementary tables

S1	List of model parameters and constants	2
----	--	---

List of supplementary figures

	S1	Linear regression fit for the parameterization of atmospheric transmissivity	3
5	S2	Linear regression fit for the parameterization of surface albedo	4
	S3	Average summer wind speeds over the lower parts of the Antarctic Ice Sheet	5
	S4	Threshold temperature for melt T_{\min}	6
	S5	Yearly total Antarctic surface melt in the historical model calibration ensemble	7
	S6	Taylor diagram summarizing the performance of the historical model calibration ensemble	8
10	S7	Present-day Antarctic surface melt rates computed with PISM using PDD	9
	S8	Surface melt rates as a function of the ice-sheet surface altitude	10
	S9	End-of-century Antarctic surface melt rates computed by dEBM-simple and comparison to RACMO	11
	S10	Melt offset M_{off}	12

Table S1. List of ice-sheet model constants and parameters used in PISM and their default values adopted for this study.

Symbol	Parameter	Value	Unit
$\Delta x, \Delta y$	Horizontal grid resolution	8	km
Δz	Vertical grid resolution	13 – 87	m
n	Glen flow law exponent	3	–
E_{SIA}	Enhancement factor for SIA	1	–
E_{SSA}	Enhancement factor for SSA	1	–
u_0	Sliding law threshold velocity (Eq. (1))	100	m yr^{-1}
q	Pseudo-plastic sliding exponent (Eq. (1))	0.75	–
c_0	Apparent till cohesion (Eq. (2))	0	Pa
ϕ_{\min}	Minimal till friction angle (Eq. (3))	2	$^{\circ}$
ϕ_{\max}	Maximal till friction angle (Eq. (3))	50	$^{\circ}$
b_{\min}	Bed elevation of ϕ_{\min} (Eq. (3))	–700	m
b_{\max}	Bed elevation of ϕ_{\max} (Eq. (3))	500	m
W_{\max}	Maximal water thickness in till (Eq. (4))	2	m
C_d	Till water drainage rate (Eq. (4))	7	mm yr^{-1}
N_0	Reference effective till pressure (Eq. (5))	1,000	Pa
e_0	Reference void ratio at N_0 (Eq. (5))	0.69	–
C_c	Till compressibility (Eq. (5))	0.12	–
δ	Lower bound of N , as fraction of overburden pressure (Eq. (5))	0.04	–
T_s	Temperature of snow precipitation	273.15	K
T_r	Temperature of rain precipitation	275.15	K
f_s	Degree-day factor for snow	3.3	$\text{mm w.e. (PDD)}^{-1}$
f_i	Degree-day factor for ice	8.8	$\text{mm w.e. (PDD)}^{-1}$
Γ	Atmospheric temperature lapse rate	–8.2	K km^{-1}
C	PICO overturning strength	1	$\text{Sv m}^3 \text{kg}^{-1}$
γ_T	PICO vertical heat exchange coefficient	$3 \cdot 10^{-5}$	ms^{-1}
K	Eigencalving coefficient	$1 \cdot 10^{16}$	ms
H_{cr}	Thickness threshold for calving	50	m

PDD, positive degree-day.

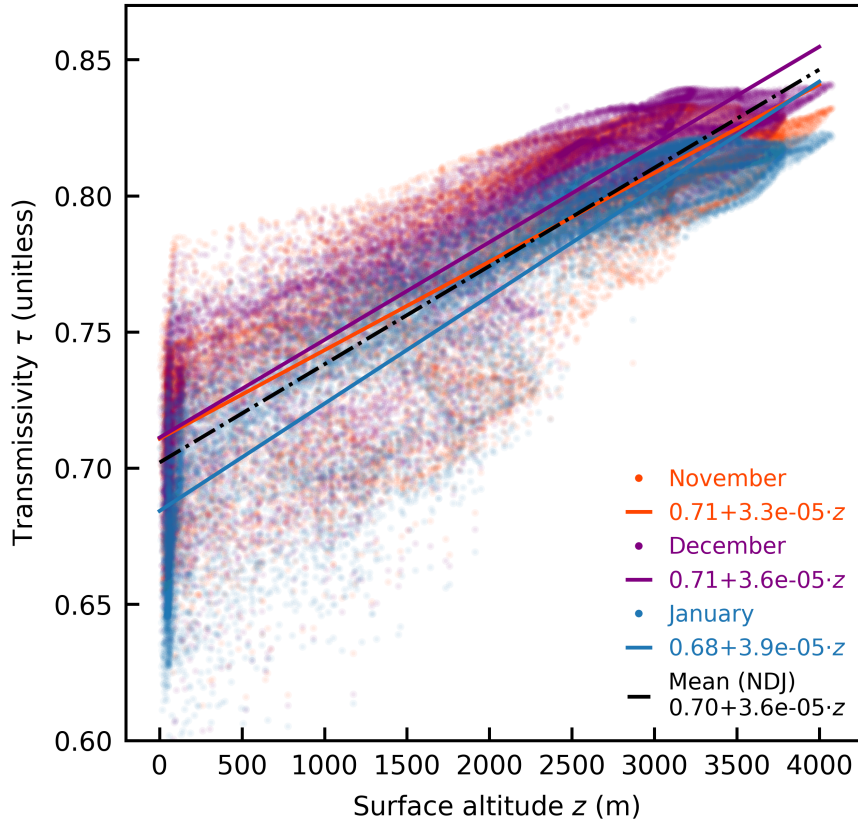


Figure S1. Linear regression fit for the parameterization of atmospheric transmissivity. Atmospheric transmissivity τ (unitless) over the Antarctic Ice Sheet versus ice-sheet surface altitude z (in m), given by multi-year monthly means of RACMO2.3p2 data over the historical period (1950–2015) computed on RACMO’s native 27 km grid. The transmissivity is calculated from the ratio of incident shortwave solar radiation at the ice surface and the top of the atmosphere (TOA). A linear regression fit is shown for each of the three austral summer months with the highest average TOA insolation (November, December and January; NDJ) (colored solid lines) with best-fit parameters given in the legend. The transmissivity parameterization in dEBM-simple (Eq. (7)) uses best-fit parameters (intercept $a_\tau = 0.70$ and slope $b_\tau = 3.6 \cdot 10^{-5} \text{ m}^{-1}$) of the linear fit resulting from the mean over those three months (gray dash-dotted line). Best-fit parameters from the November, December and January regression fits serve as uncertainty estimates in the model sensitivity ensemble (Sect. 5.3).

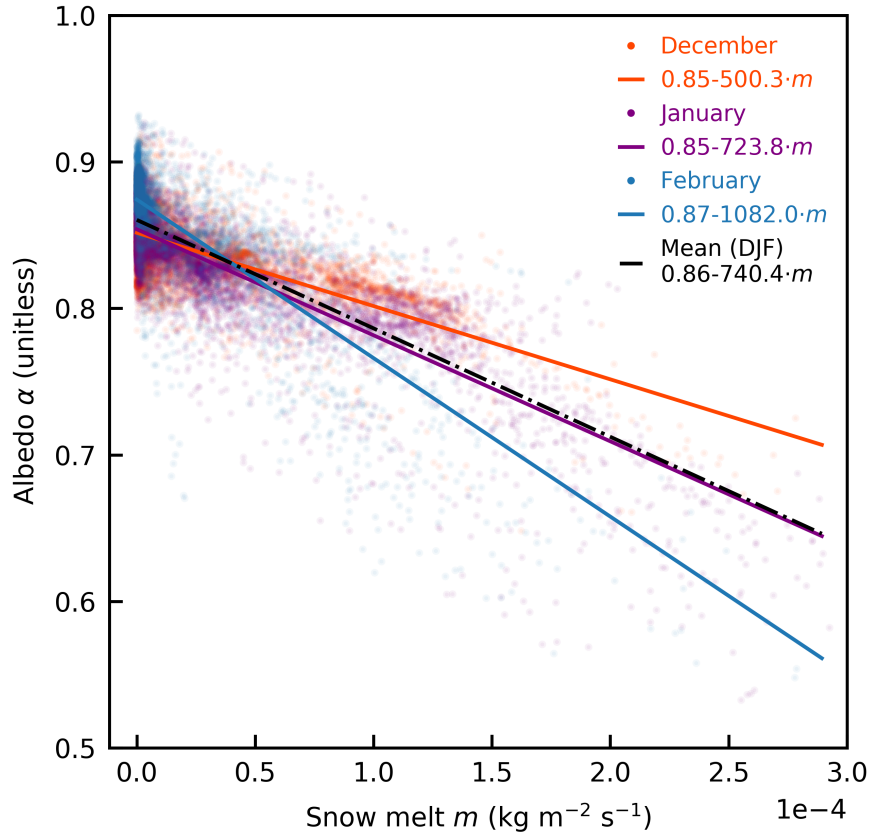


Figure S2. Linear regression fit for the parameterization of surface albedo. Antarctic surface albedo α (unitless) versus snow melt m (in $\text{kg m}^{-2} \text{s}^{-1}$), given by multi-year monthly means of RACMO2.3p2 data over the period 2085 to 2100 under the SSP5-8.5 warming scenario provided by CESM2, computed on RACMO’s native 27 km grid. A linear regression fit is shown for each of the three austral summer months with the highest average melt (December, January, February; DJF) (colored solid lines) with best-fit parameters given in the legend. The albedo parameterization in dEBM-simple (Eq. (8)) uses best-fit parameters (intercept $a_\alpha = 0.86$ and slope $b_\alpha = -740.4 (\text{kg m}^{-2} \text{s}^{-1})^{-1}$) of the linear fit resulting from the mean over those three months (gray dash-dotted line). Best-fit parameters from the December, January and February regression fits serve as uncertainty estimates in the model sensitivity ensemble (Sect. 5.3). Grid cells where the mean albedo is below the allowed minimum value $\alpha_{\min} = 0.47$ and grid cells which show melt even below the allowed minimum temperature $T_{\min} = -10^\circ\text{C}$ have been masked before the fits.

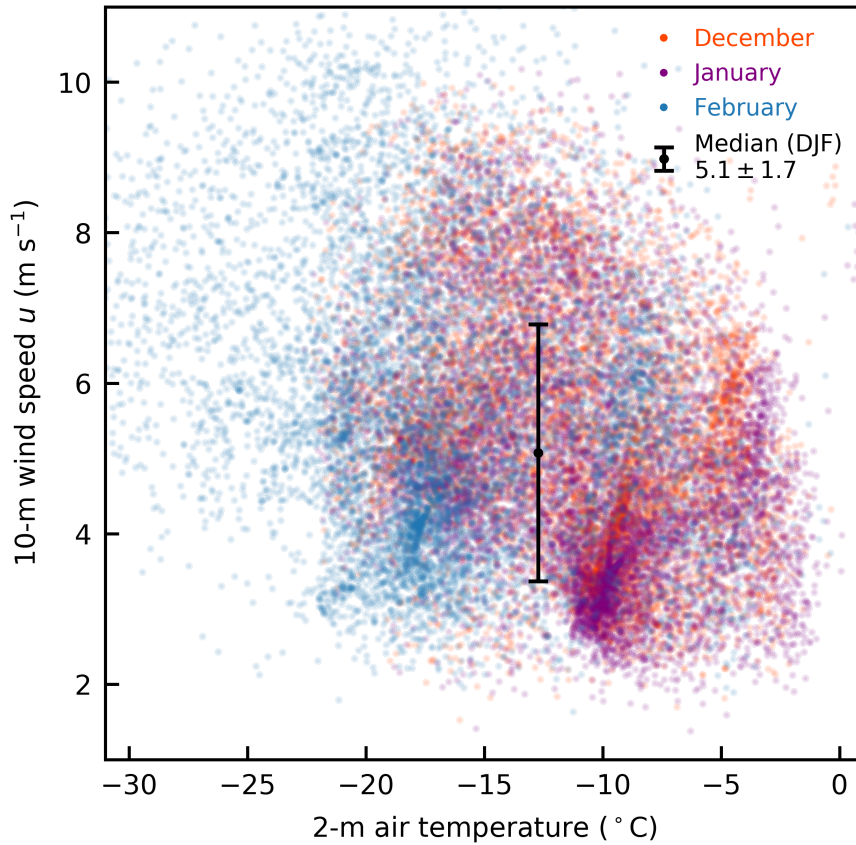


Figure S3. Average summer wind speeds over the lower parts of the Antarctic Ice Sheet. Wind speed at 10 m above ground u (in m s^{-1}) during the austral summer months December, January and February (DJF) over the lower parts of the Antarctic Ice Sheet (elevations $< 2,000$ m) versus near-surface (2 m) air temperature (in $^{\circ}\text{C}$), given by multi-year monthly means of RACMO2.3p2 data over the historical period (1950–2015), computed on RACMO’s native 27 km grid. The black dot marks the DJF median (value given in the legend) that is used in the estimation of the dEBM-simple tuning parameter c_1 for the best-guess value. The error bars denote the standard deviation.

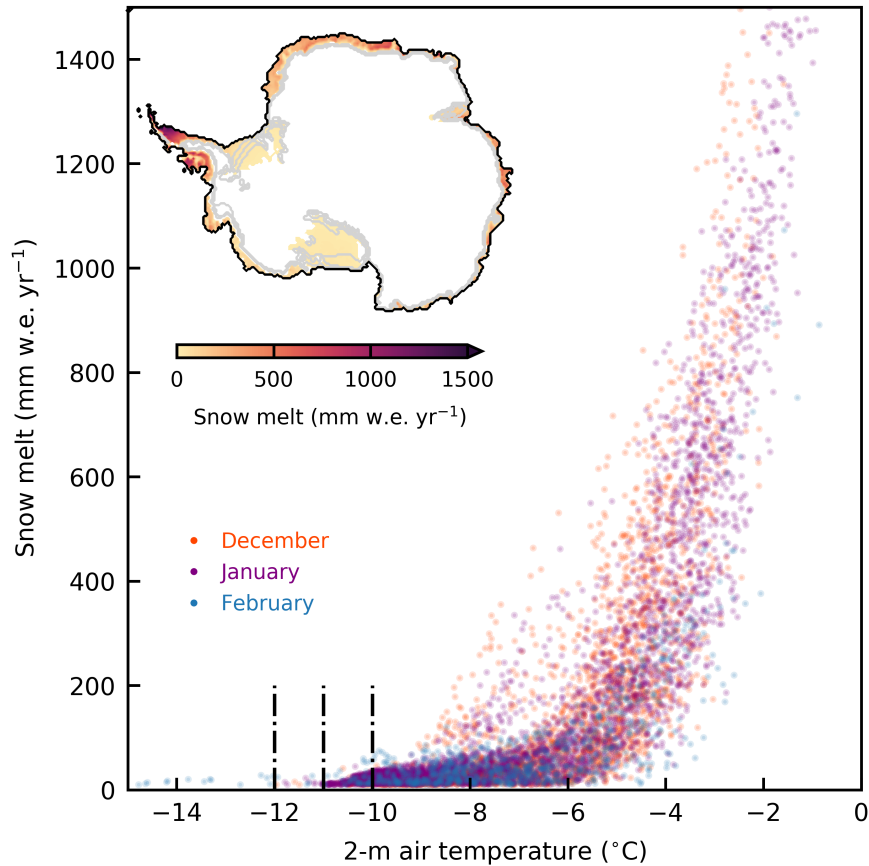


Figure S4. Threshold temperature for melt. Antarctic snow melt rates (in millimeters water equivalent per year, mm w.e. yr^{-1}) as a function of near-surface air temperature (in $^{\circ}\text{C}$), given by multi-year monthly means of RACMO2.3p2 data over the historical period (1950–2015) for the austral summer months with the highest average melt (December–February; DJF), computed on RACMO’s native 27 km grid. The black dash-dotted lines mark the temperature values that are used in the calibration as estimates of the threshold temperature T_{min} , which constitutes the background melt condition in dEBM-simple. They mark the approximate long-term monthly mean temperature range above which significant surface melt occurs in the RACMO simulations. The inset shows a map of the spatial distribution of 1950 to 2015 multi-year mean DJF Antarctic snow melt rates from RACMO. The gray contour lines mark the -10 , -11 , -12 $^{\circ}\text{C}$ isotherms of long-term mean summer air temperatures (1950–2015 DJF mean), respectively, that roughly approximate the mean extent of the melt area.

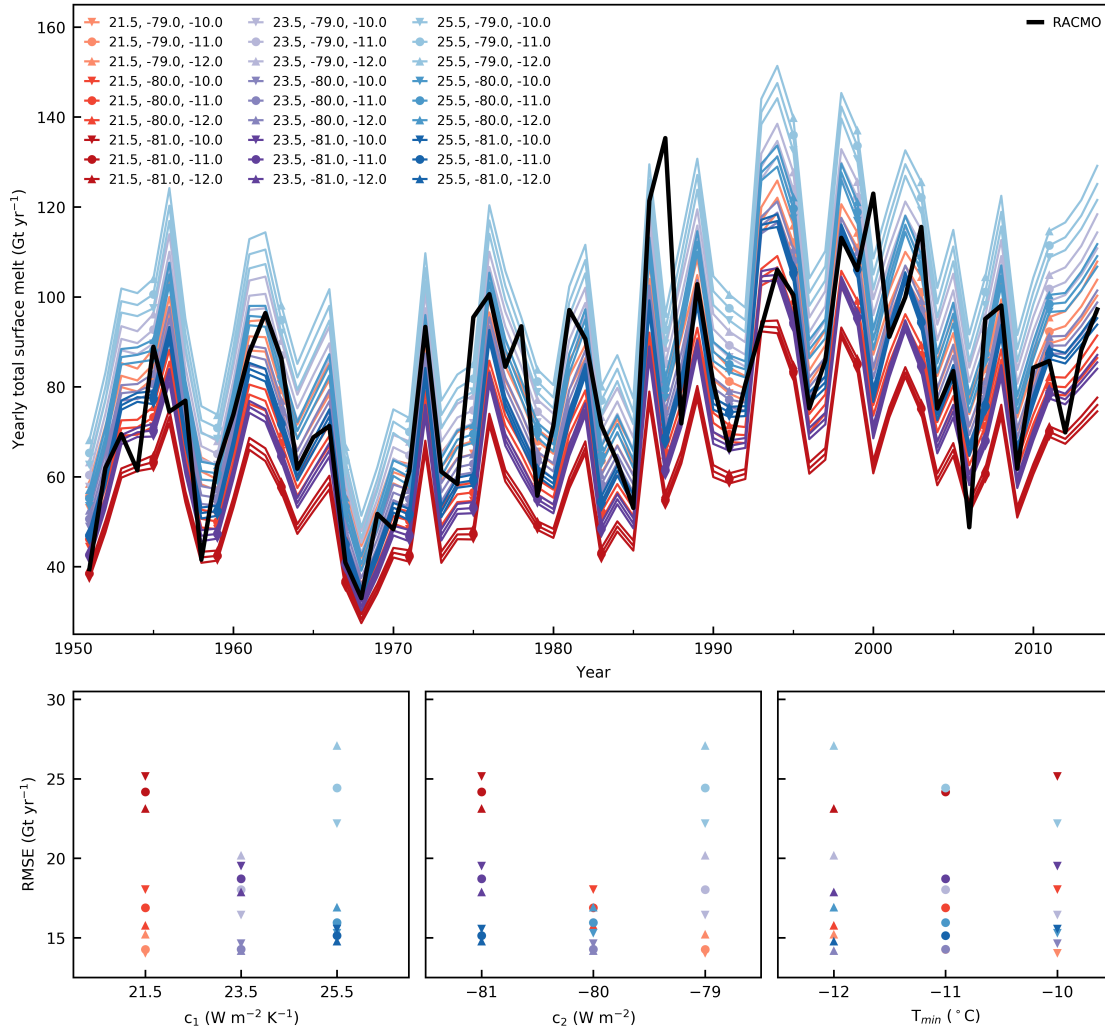


Figure S5. Yearly total Antarctic surface melt in the historical model calibration ensemble. Upper panel shows the evolution of Antarctic-wide integrated yearly total surface melt flux (in gigatons per year, Gt yr^{-1}) as calculated with PISM-dEBM-simple in the historical (1950–2015) model calibration ensemble using a fixed geometry (colored lines). The number tuples in the legend are $\{c_1$ (in $\text{W m}^{-2} \text{K}^{-1}$), c_2 (in W m^{-2}), T_{\min} (in $^{\circ}\text{C}$)}. The black line shows the yearly total surface melt flux derived with RACMO2.3p2 under boundary forcing from CESM2, regridded to PISM’s 8 km grid using the same surface mask. Lower panels show the respective temporal root-mean-square error (RMSE, in Gt yr^{-1}) of each model ensemble member with respect to RACMO, individually plotted against c_1 (left), c_2 (middle), and T_{\min} (right).

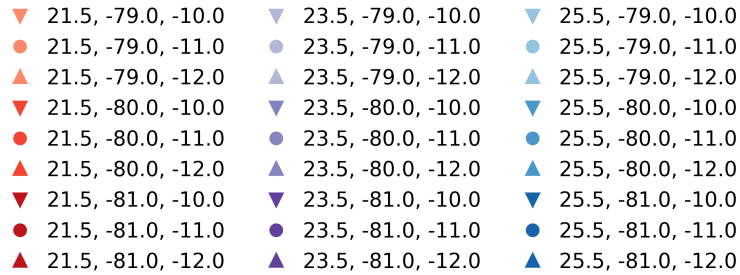
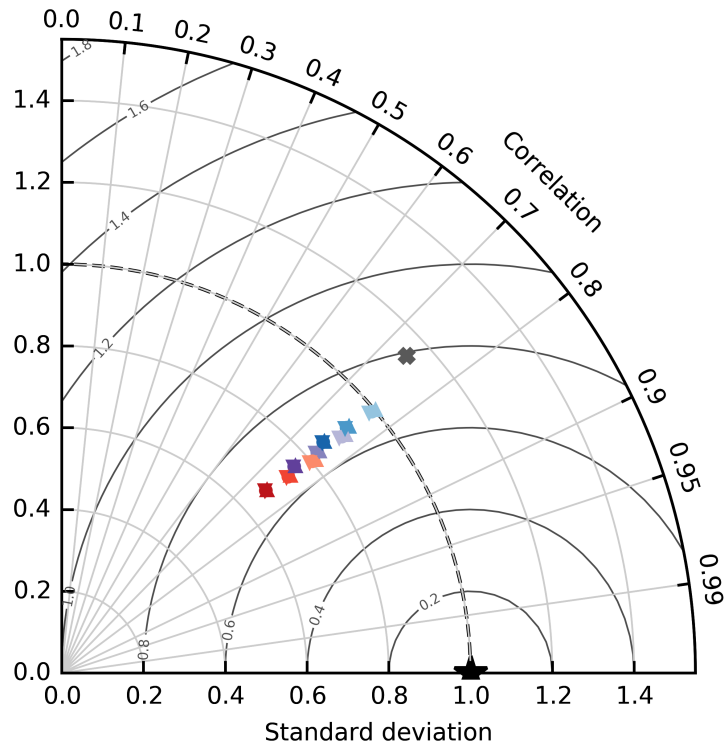


Figure S6. Taylor diagram summarizing the performance of the historical model calibration ensemble. The diagram shows a summary of the performance of each ensemble member from the historical model calibration ensemble (colored markers; legend entries as in Fig. S5) compared to the Antarctic-wide integrated yearly total surface melt flux from RACMO2.3p2 (black pentagram). The horizontal and vertical axes represent the standard deviation, normalized with respect to the standard deviation of the RACMO surface melt flux (bold dashed black line). The azimuthal angle shows the correlation between the individual ensemble members and RACMO, given by the Pearson correlation coefficient. Finally, the (normalized) centered root-mean-square error, representing a bias-corrected equivalent of the root-mean-square error, is given by the circular dark gray contour lines. The gray cross marker shows the performance of PISM using the standard PDD scheme for comparison.

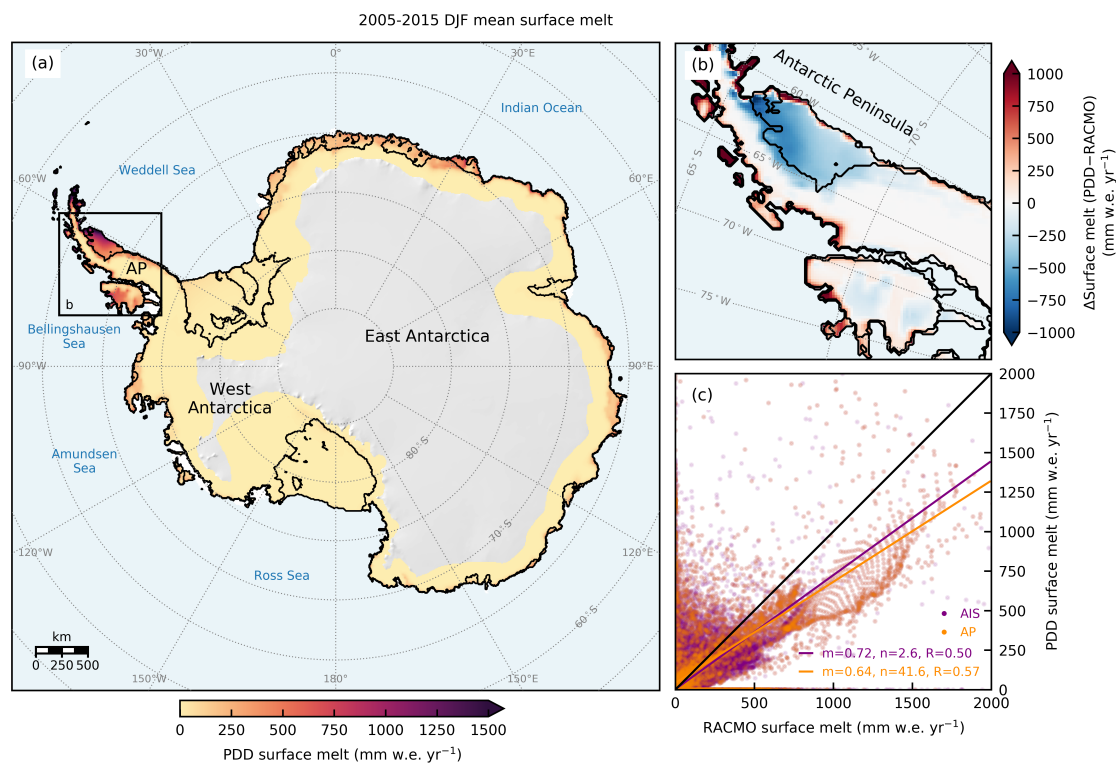


Figure S7. Present-day Antarctic surface melt rates computed with PISM using PDD. Same as Fig. 2, but for PDD. (a) Map of Antarctic mean 2005–2015 summer (December–February; DJF) surface melt rates (in mm w.e. yr⁻¹), as calculated with PISM using a standard PDD scheme. Areas with melt rates below numerical significance (<0.001 mm w.e. yr⁻¹) are masked. AP, Antarctic Peninsula. (b) Absolute difference of PDD minus RACMO2.3p2-computed surface melt rates (in mm w.e. yr⁻¹), averaged over the same period and shown for a zoomed-in section of the Antarctic Peninsula (indicated by the black square in panel (a)). (c) Scatter plot of PDD versus RACMO-computed summer surface melt rates (in mm w.e. yr⁻¹) and linear regression fits of the data (colored solid lines). Purple data points correspond to the whole Antarctic Ice Sheet (AIS), orange data points to the zoomed-in section of the AP shown in panel (b). The black line marks the identity line.

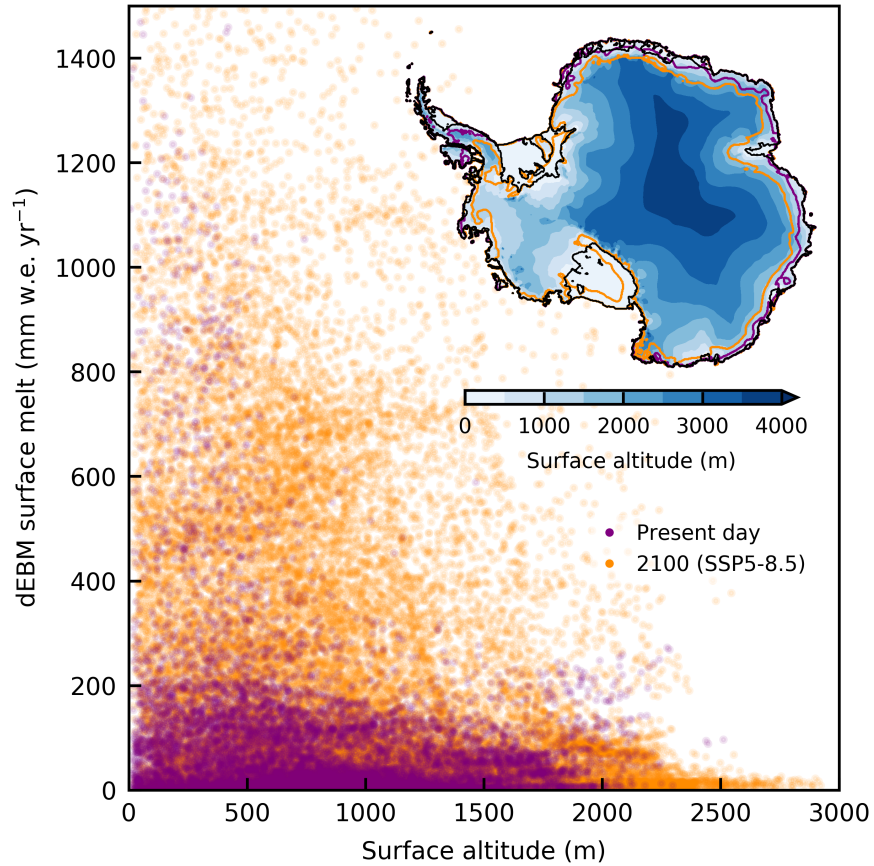


Figure S8. Surface melt rates as a function of the ice-sheet surface altitude. Antarctic surface melt rates (in mm w.e. yr⁻¹) over the grounded parts of the ice sheet as computed with PISM-dEBM-simple, shown as a function of ice-sheet surface altitude for present day (year 2015; purple data points) and the year 2100, assuming an SSP5-8.5 atmospheric warming scenario (orange data points). The inset map shows the maximum extent of the melt area at the two respective times as colored contours, overlaid on the present-day ice-sheet surface altitude (contour levels of 500 m).

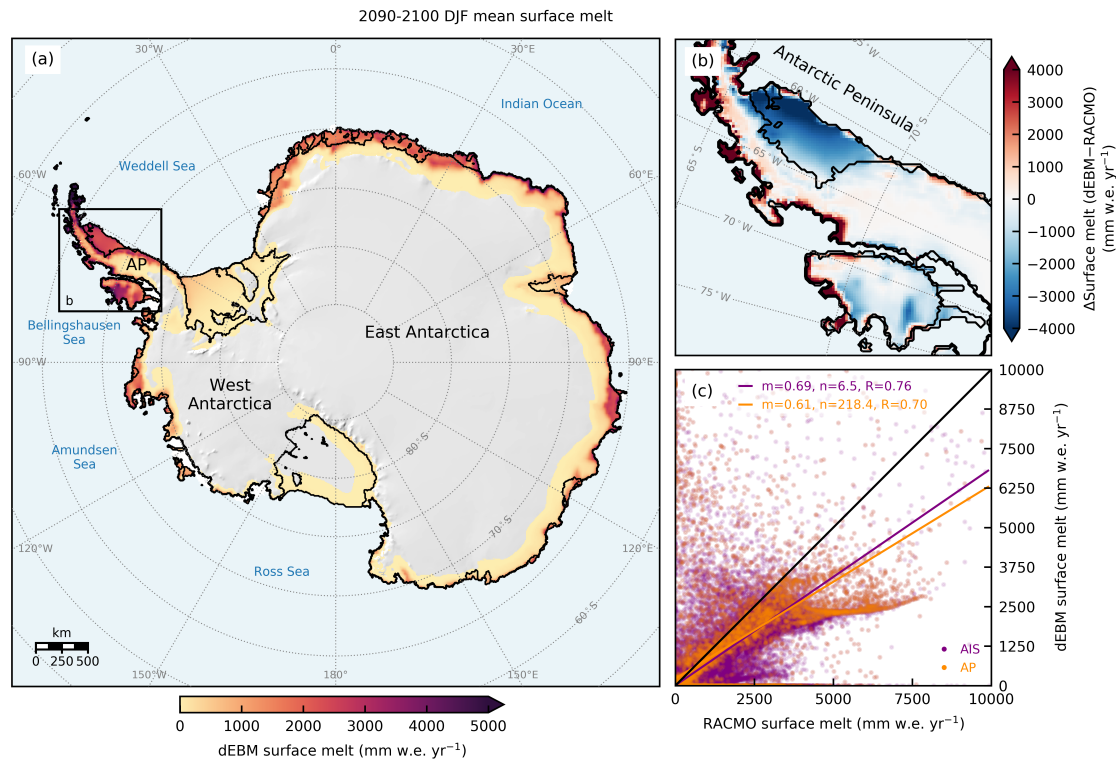


Figure S9. End-of-century Antarctic surface melt rates computed by dEBM-simple and comparison to RACMO. Same as Fig. 2, but for the period 2090–2100, following an SSP5-8.5 warming scenario. (a) Map of Antarctic mean 2090–2100 summer (December–February; DJF) surface melt rates (in mm w.e. yr⁻¹), as calculated with PISM-dEBM-simple in the calibrated 21st-century projection run forced by RACMO2.3p2 with atmospheric boundary forcing from CESM2 and following an SSP5-8.5 warming scenario. Areas with melt rates below numerical significance (<0.001 mm w.e. yr⁻¹) are masked. AP, Antarctic Peninsula. (b) Absolute difference of dEBM-simple minus RACMO-computed surface melt rates (in mm w.e. yr⁻¹), averaged over the same period, shown for a zoomed-in section of the Antarctic Peninsula (indicated by the black square in panel (a)). (c) Scatter plot of dEBM-simple versus RACMO-computed summer surface melt rates (in mm w.e. yr⁻¹) and linear regression fits of the data (colored solid lines). Purple data points correspond to the whole Antarctic Ice Sheet (AIS), orange data points to the zoomed-in section of the AP shown in panel (b). The black line marks the identity line. Note that the axis limits in all panels are different from those in Fig. 2.

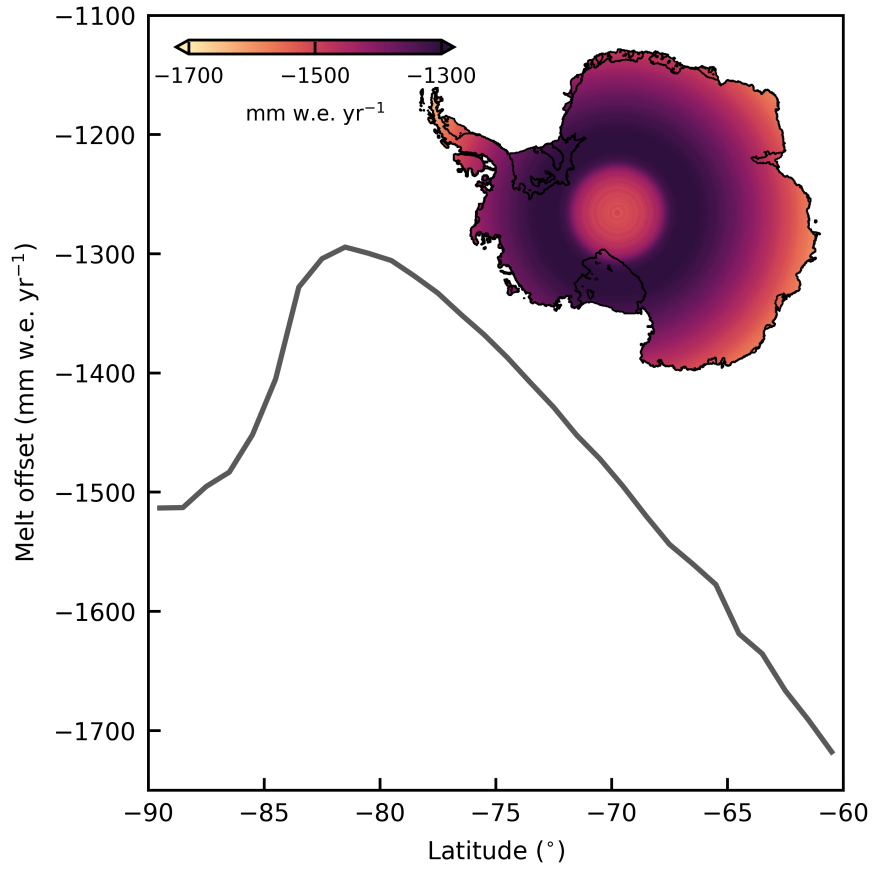


Figure S10. Melt offset M_{off} . Annual average surface melt potential $M_{\text{off}} \propto c_2$ (in mm w.e. yr⁻¹) resulting from outgoing longwave radiation (third term in Eq. (6)), which acts as a negative contribution (offset) to the total surface melt flux, as a function of latitude. Inset map shows the spatial distribution.